Proceedings of IDETC/CIE 2006
ASME 2006 International Design Engineering Technical Conferences &
Computers and Information in Engineering Conference
September 10-13, 2006, Philadelphia, Pennsylvania, USA

DETC2006-99727

DESIGN OF A STATICALLY BALANCED TENSEGRITY MECHANISM

Mark Schenk, Just L. Herder*
BioMechanical Engineering
Mechanical, Maritime and Materials Engineering
Delft University of Technology
Mekelweg 2, 2628 CD, Delft
The Netherlands
Email: J.L.Herder@3me.tudelft.nl

Simon D. Guest
Department of Engineering
University of Cambridge
Trumpington Street
Cambridge CB2 1PZ
United Kingdom
Email: sdg@eng.cam.ac.uk

ABSTRACT

The combination of static balancing and tensegrity structures has resulted in a new class of mechanisms: Statically Balanced Tensegrity Mechanisms. These are prestressed structures that are in equilibrium in a wide range of positions, and thus exhibit mechanism-like properties. This paper describes the design of a prototype model of a statically balanced tensegrity mechanism based on a classic tensegrity structure.

INTRODUCTION

On the border between structures and mechanisms, we find a new and special class of structures termed *Statically Balanced Tensegrity Mechanisms*. These result from the combination of the fields of *static balancing* and *tensegrity structures*. Statically balanced systems are in equilibrium in every configuration in their workspace, and as they require little to no effort to operate, they are used for energy-efficient design in for instance robotics and medical settings (see Fig. 1) [1]. A common element in static balancing is the use of zero-free-length springs, i.e. springs that are pretensioned such that, in their working range, their tension is proportional to their length. The utility of zero-free-length springs was initially exploited in the design of the classic 'Anglepoise' lamp [2], but is more generally applied in the field of static balancing, and its properties are a prerequisite for the construction of statically balanced tensegrity mechanisms.

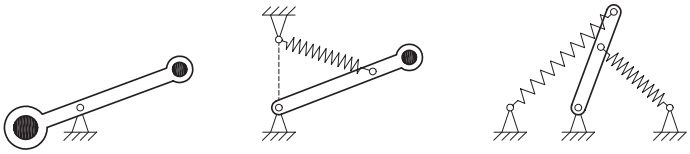

Figure 1. Static balancing: the three structures shown are in equilibrium for any position of the bar, as long as in (a) the masses (black circles) are correctly chosen, and in (b) and (c) the springs are zero-free-length springs with appropriately chosen stiffness.

Tensegrity structures, or tensegrities, are a special type of prestressed pin-jointed bar frameworks with unique properties: the tension elements are usually replaced by cables, resulting in aesthetic, light-weight structures that seem to defy gravity [3–6]. The structures are generally both statically and kinematically indeterminate, meaning they are self-stressed and have internal mechanisms – displacements that to first order do not change member lengths. The structures derive their stiffness from the state of self-stress, which may stabilize any internal mechanisms present [7]. Conventionally, tensegrity structures are designed to be as stiff as possible. Here we employ them as mechanisms by replacing the tension members with appropriate zero-free-length springs. As a result the tensegrity structures become statically balanced, i.e. they are in equilibrium over a continuous range of positions, they are neutrally stable, and have zero stiffness [8].

*Address all correspondence to this author.

The distinguishing feature of these mechanisms is that they are pretensioned, i.e. every member carries a non-zero axial load, and although member lengths and orientations change during displacement, they remain in equilibrium and thus require no external work to deform.

This paper will describe the design of such a statically balanced tensegrity mechanism based on a classic tensegrity structure, and will discuss the required steps in the design process: equilibrium conditions, zero stiffness analysis, and range of motion. A prototype mechanism was built, and particular focus will be placed on the (novel) aspects associated with this type of structure, which arose during design and construction.

MECHANISM SYNTHESIS AND ANALYSIS

The statically balanced tensegrity mechanisms described in this paper are at once both prestressed structure and mechanism: they continuously remain in equilibrium under the internal tensions, throughout a large range of motion. This is also what sets their synthesis and analysis apart from conventional mechanisms.

The theory of statically balanced tensegrity mechanisms, or, equivalently, zero stiffness tensegrity structures, was investigated by [8] using the tools of structural engineering and mathematical rigidity theory, e.g. [9]. It was described why and when structures have zero stiffness, if zero-free-length springs are introduced. Additionally it was theoretically shown that the relevant zero-stiffness modes are valid over finite displacements, i.e. are indeed mechanisms. However, the tools of structural engineering are ill-equipped to deal with mechanisms, as they only consider infinitesimal deviations from an initial equilibrium configuration. The structures described here do not have a preferred position, and as the zero stiffness results in singular stiffness matrices, iterative approximative techniques have to be employed to calculate displacements. Therefore, a different approach is desired to analyse the mechanism properties. The method currently used is to derive the analytical equilibrium equations, and use those to describe the equilibrium path. This is only practically possible for relatively simple structures, which can be described with few (generalized) parameters. Even then, not the entire behaviour can be described, as will be illustrated by the example structure.

The synthesis of the statically balanced tensegrity mechanisms will not be discussed in this paper, but we will instead focus on the analysis of a structure shown to be a statically balanced tensegrity mechanism [8], using analytical equilibrium conditions to analyse some aspects of the mechanism properties.

PROTOTYPE ANALYSIS

The structure chosen for the construction of the prototype model, is a classic tensegrity structure, as shown in Fig. 2. It is a spatial structure consisting of three bars and nine cables. When constructed with conventional elements, the structure derives its stiffness from the self-stress in the system, as there exists an infinitesimal internal mechanism. Consequently, it would feel a bit 'soft' in some directions.

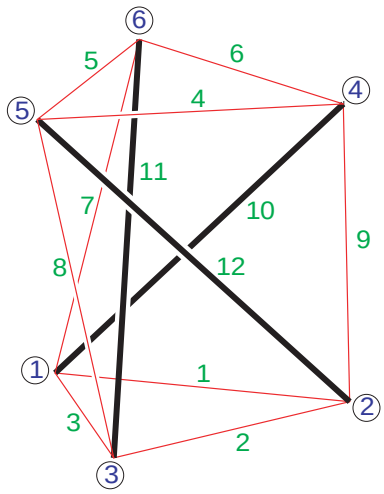

Figure 2. Rotationally symmetric tensegrity structure. The structure has a circumscribing radius r, height h and the two parallel equilateral triangles (nodes 1–3 and nodes 4–6) are rotated $\pi/6$ with respect to each other.

When replacing all wires by appropriately chosen zero-free-length springs, the structure will have zero stiffness, i.e. it will be statically balanced. The presence of zero-stiffness modes in tensegrity structures can be predicted using the theory described in [8]: the structure at hand will have three zero-stiffness modes, i.e. three independent statically balanced displacements.

This section will first describe the equilibrium conditions, followed by the structural analysis, showing that the structure indeed has no stiffness in certain modes, and is thus a mechanism.

Equilibrium analysis

In tensegrity literature, finding an equilibrium position is referred to as *form finding*, and many techniques have been developed [10]. The structure used for the prototype is the simplest member of a class of rotationally symmetric prismic tensegrities. For this class, analytical solutions are available and generally two approaches can be distinguished: working from nodal equilibrium at each of the nodes (static approach), or by making use of the property of tensegrities that the cables reach a minimum and the bars a maximum length in the equilibrium configuration (kinematic approach). In Appendix A a full derivation is provided using the static approach.

The results yield several interesting properties: the twist angle α between top and bottom polygons, is independent of their circumscribing radius r or the height h of the structure, and is

merely a function of the number of vertices n of the polygons:

$$\alpha = \frac{\pi}{2} - \frac{\pi}{n} \tag{1}$$

In our case, with three bars, the triangles are thus twisted $\pi/6$ with respect to each other. For a structure with equal top and bottom radius r, bar length b, and vertical cable length l, the tensions are given by

$$\begin{bmatrix} t_v & t_h \end{bmatrix} = -\frac{t_b}{b}\begin{bmatrix} l & r \end{bmatrix} \tag{2}$$

with t_v, t_h and t_b respectively the tension in the vertical cables, horizontal cables and bars. This becomes interesting when rewritten in terms of *force density* or *tension coefficient*

$$\hat{t}_v = -\hat{t}_b \tag{3}$$

$$\hat{t}_v = 2\sin\left(\frac{\pi}{n}\right)\hat{t}_h \tag{4}$$

where the tension coefficient $\hat{t}$ is defined as the tension t in the member divided by the length l, $\hat{t} = \frac{t}{l}$. Note that for zero-free-length springs it is equal to the spring stiffness, $K_{zfl} = \frac{t}{l}$, and thus when replacing the cables by the zero-free-length springs, the vertical springs of the prototype should be $2\sin\left(\frac{\pi}{3}\right) = \sqrt{3}$ times stiffer than the horizontal ones.

Now, if the structure is deformed symmetrically, while maintaining the same ratio between bottom and top radius of the structure, the tension coefficients remain constant. As the spring stiffness of a zero-free-length spring is equal to its tension coefficient, the prototype structure will then remain in equilibrium, provided that the tension coefficient of the bar also remains constant. That is true if the bar length (and thus tension) is invariant. This behaviour corresponds to the theory developed in [8], and is a common property of statically balanced tensegrity mechanisms: only the lengths of zero-free-length springs change.

Note that the equilibrium of the structure is modelled under absence of external loads, and hence when constructed with the zero-free-length springs would collapse under its own weight. In the demonstration model this is countered by the friction forces present.

Structural analysis

The structure was analysed for its stiffness modes in an arbitrary initial position, using the tangent stiffness matrix of the structure. The tangent stiffness matrix $\mathbf{K}_t$ is a common component in structural analysis, and relates infinitesimal displacements $\mathbf{d}$ to force perturbations $\mathbf{f}$

$$\mathbf{K}_t\mathbf{d} = \mathbf{f} \tag{5}$$

As the tangent stiffness matrix is well-known in structural analysis, many different formulations for it exist, e.g. [11, 12]. Different formulations with identical underlying assumptions will produce identical numerical results, but may provide a different *understanding* of the stiffness. The formulation used in this paper is derived by [13], and incorporates large strains. It is written as

$$\begin{aligned} \mathbf{K}_t &= \hat{\mathbf{K}} + \mathbf{S} \\ &= \mathbf{A}\hat{\mathbf{G}}\mathbf{A}^T + \mathbf{S} \end{aligned} \tag{6}$$

where $\mathbf{S}$ is the *stress* matrix, $\hat{\mathbf{K}}$ is the *modified material stiffness matrix*, $\mathbf{A}$ is the *equilibrium matrix* for the structure and $\hat{\mathbf{G}}$ is a diagonal matrix whose entries consist of the *modified axial stiffness* for each of the members. The modified axial stiffness $\hat{g}$ is defined as

$$\hat{g} = g - \hat{t} \tag{7}$$

where g is the conventional axial stiffness and $\hat{t}$ the tension coefficient. For conventional members, $\hat{g}$ will be little different from g. It will certainly always be positive, and hence the matrix $\hat{\mathbf{G}}$ will always be positive definite. However, for a zero-free-length spring, because the tension t is proportional to the length, $t = gl$, the tension coefficient is equal to the axial stiffness, $\hat{t} = t/l = g$, and the modified axial stiffness $\hat{g} = g - \hat{t} = 0$. Thus structures constructed with zero-free-length springs will have zeros along the diagonal of $\hat{\mathbf{G}}$ corresponding to these members, and $\hat{\mathbf{G}}$ will now only be positive *semi*-definite. It is this consequence of the use of zero-free-length springs, that causes the structures to exhibit zero stiffness.

This derivation of the tangent stiffness matrix differs from the commonly used formulations in that it does not explicitly distinguish between the material stiffness and geometric stiffness of the structure. Instead it combines part of the geometric stiffness matrix with the material stiffness, by introducing the modified axial stiffness. This approach was crucial in introducing zero-free-length springs to structural analysis. The resulting stress matrix represents the state of self-stress (it only contains tension coefficients) which may stabilize the internal mechanisms in the structures.

Example analysis. The structure in Fig. 2 was analysed with $r = 1$ and $h = 2$. All conventional elements have an 'axial stiffness' of $EA = 100$N, the horizontal springs 1N/m and the vertical springs $\sqrt{3}$N/m. The internal tension of the structure is uniquely prescribed by these spring stiffnesses. The axial stiffness was chosen this low to prevent numerical noise, and is possible because the actual stiffness is irrelevant as the bar lengths remain constant in the zero-stiffness modes [8].

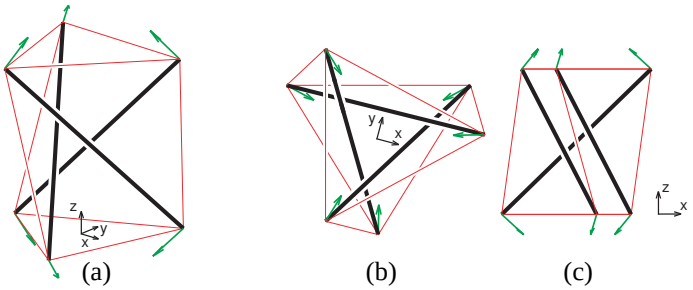

Figure 3. Fully symmetric zero-stiffness mode, with (a) 3D view, (b) top view and (c) side view. All displacement vectors are of equal magnitude, and with equal z-component. In this mode the rotation angle between bottom and top triangle remains constant throughout the displacement.

The tangent stiffness of the structure has been found using the formulation of Eqn. 6 for two different cases. Firstly, with the structure consisting of conventional elements, and secondly, when made from conventional compressive bars, but using zero-free-length springs as tension members. The level of self-stress – and thus the stress matrix – is identical for both cases. The results are presented as the stiffness of each of the eigenmodes (excluding rigid-body motions) in Tables 1(a) and 1(b).

Table 1. Stiffness of each of the eigenmodes, excluding rigid-body motions, for (a) the conventional structure and (b) the structure with zero-free-length springs as tension members. The total stiffness $\mathbf{K}_t$ is the sum of the contributions of $\hat{\mathbf{K}}$ and $\mathbf{S}$.

(a)			(b)		
$\mathbf{K}_t$	$\hat{\mathbf{K}}$	$\mathbf{S}$	$\mathbf{K}_t$	$\hat{\mathbf{K}}$	$\mathbf{S}$
5.630	0.017	5.613	0.000	0.000	0.000
27.838	26.196	1.642	0.000	0.000	0.000
27.838	26.196	1.642	0.000	0.000	0.000
83.219	79.195	4.023	5.670	0.026	5.643
83.219	79.195	4.023	5.670	0.026	5.643
107.376	103.074	4.301	5.789	0.017	5.772
107.376	103.074	4.301	6.000	0.000	6.000
113.852	113.535	0.317	6.000	0.000	6.000
132.506	130.474	2.032	6.000	0.000	6.000
132.506	130.474	2.032	75.599	75.372	0.227
176.205	170.205	6.000	75.719	75.362	0.356
225.457	225.388	0.069	75.719	75.362	0.356

For the conventional structure all eigenvalues of the tangent stiffness matrix are positive, and the stress matrix is of maximal rank. The system has an internal mechanism, which is stabilized by the state of self-stress. This can be seen in the first line of Tab. 1(a), where the $\hat{\mathbf{K}}$ component is almost zero (it is not precisely zero because the eigenvectors of $\hat{\mathbf{K}}$ and $\mathbf{K}_t$ are not precisely aligned).

When zero-free-length springs are placed in the structure, three new zero-stiffness modes appear in $\mathbf{K}_t$ – the first three rows of Tab. 1(b). These modes can be considered in a symmetry-adapted form [14] as a totally symmetric mode, and a pair of modes that are symmetric and antisymmetric with respect to a dihedral rotation. The fully symmetric mode is shown in Fig. 3. It corresponds to a mode where the structure is compressed in the x-y plane and expands in the z-direction (or vice versa).

Mechanism analysis

The next step is to translate the results from the structural analysis, which are infinitesimal displacements, into actual mechanism information. In [8] it was argued theoretically that the type of zero-stiffness modes found in the numerical analysis are indeed finite, but the question stands how they are best interpreted over a large range of motion. For the example structure, the analytical equilibrium solutions were used to analyse the fully symmetric deformation shown in Fig. 3. The two other zero-stiffness modes, however, cannot be analysed with the same approach, and therefore the more general problem remains: the current design approach allows the synthesis of tensegrity structures, and allows to predict and numerically confirm the number of zero-stiffness modes, but understanding the precise properties of the mechanism is currently limited to analytical solutions.

The analysis of the prototype structure is done by increasing the height of the structure stepwise, and by rewriting Eqn. A.2, under the assumption of a constant bar length and identical radius for top and bottom polygon, the corresponding radius can be found:

$$r = \sqrt{\frac{b^2 - h^2}{2 - 2\cos(2\pi/n + \alpha)}} \tag{8}$$

This analysis is possible, because the bar lengths remain constant throughout the displacement. Note that the twist angle α of the structure also remains constant throughout this deformation mode. The range of motion is then expressed in terms of the normalized parameter h/r, which is the ratio of the height over the radius. Translating the h/r ratio into actual values of height and radius, is done by means of Fig. 4. Along the vertical axes usually other normalized parameters are plotted, and in general the values need to be multiplied with the bar length to obtain the actual values for a given structure.

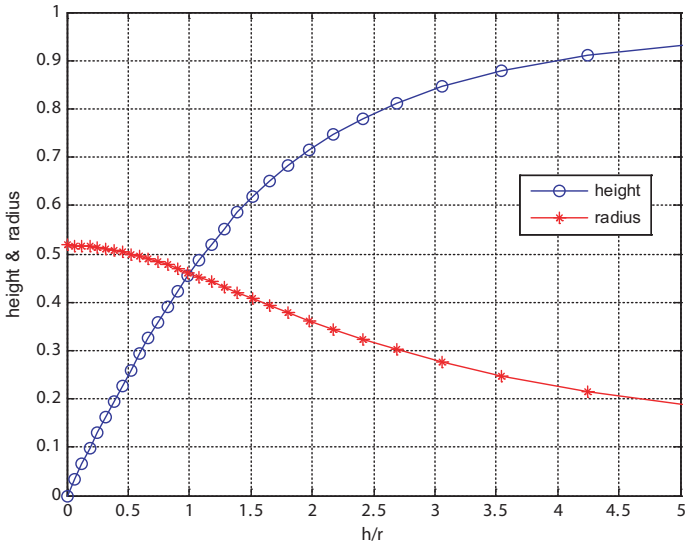

Figure 4. Height and radius of the structure, for a given h/r ratio. To obtain actual values, multiply by the bar length of the structure.

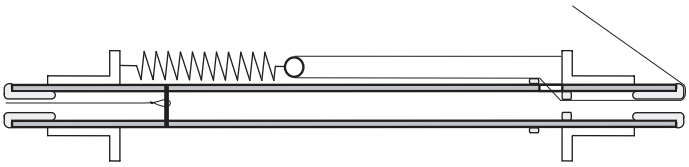

Figure 5. Conceptual design of the bars of the tensegrity mechanism, in cross-section view. Only one spring is shown, but two more are attached in a similar manner, along the circumference of the flanges. Note that this image is not to scale.

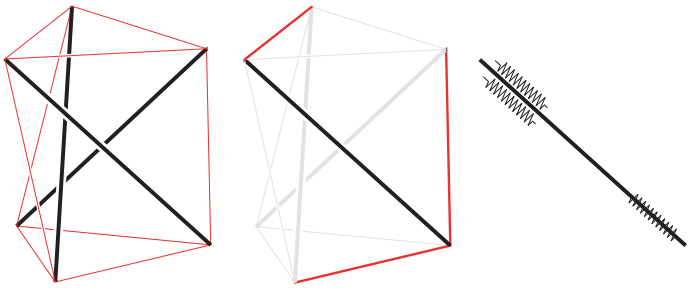

Figure 6. The three springs corresponding to each bar: two springs (vertical and horizontal) are attached on one end, and one (horizontal) on the other.

PROTOTYPE DESIGN

A (qualitative) design description is first given, before the dimensions and the range of motion of the structure are determined. The choice of bar length and dimensions of the other components proved to be very much intertwined with the possible range of motion.

Design description

For the static balancing of the tensegrity structure, the use of springs with a zero rest length is a condition *sine qua non*. However, the prototype does not actually feature pretensioned zero-free-length springs, and their properties are emulated by means of regular non-pretensioned springs. This choice is motivated by the manufacturing difficulties of zero-free-length springs, and the physical rest length of the springs which would unnecessarily limit the range of motion of the structure. The properties of the zero-free-length spring are emulated by running the wire over the endpoint of the bar, to a conventional spring [1]. By correctly choosing the total wire length, the spring will be at its rest length when the endpoint of the wire coincides with the endpoint of the bar, and thus the tension will be proportional to the 'length' of the wire between the two bars it connects.

This translates into a design (schematically shown in Fig. 5) where wires run over a yarn guide on the endpoint of the bar, wrap around a pulley attached to the spring, and are fixed at a flange. This pulley construction halves the necessary elongation of the spring. The other end of the wire is attached to a pin inside the other bar. As the total structure consists of three bars and nine springs (three vertical and six horizontal), each bar therefore has three springs attached: a 'horizontal' and 'vertical' spring on one end, and a 'horizontal' on the other (see Fig. 6).

An important part of the design is the correct choice of the springs. Unlike in many spring applications, the precise spring stiffness is not relevant in statically balanced tensegrity mechanisms, as the springs balance each other out. A crucial property of the springs, however, is the required spring stiffness ratio between the horizontal and vertical springs as calculated in Appendix A: the vertical spring must be $\sqrt{3}$ times stiffer than the horizontal spring. From a practical perspective there are more requirements to the springs. First of all, the springs need to be able to reach a high level of elongation to achieve a maximal working range. Also, most off-the-shelf springs are pretensioned to some degree. Not only does this complicate assembly as it has to be taken into account for the wire lengths, but the pretension would also limit the working range of the mechanism as the force/displacement relationship is cut off sharply when the spring reaches its rest length. For these reasons custom-made springs without pretension were used. To compensate for manufacturing imperfections, and to allow individual tuning of the springs to obtain the properties of a zero-free-length spring, adjustment of the spring position and wire length was possible.

If perfectly constructed (i.e. friction free, and true zero-free-length springs) the structure would collapse under its own weight, and the aim therefore was to minimize the weight, and thus size, of the structure. In the following section a minimum bar length is determined which, given the constraints imposed by the components, provides a certain desired working range.

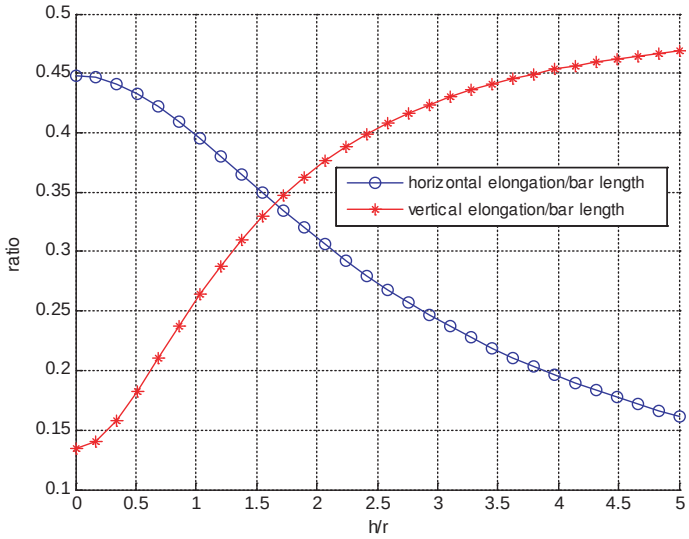

Figure 7. Elongation of springs as ratio of bar length. As a result of the use of the pulleys, it is half of the length of the corresponding wire.

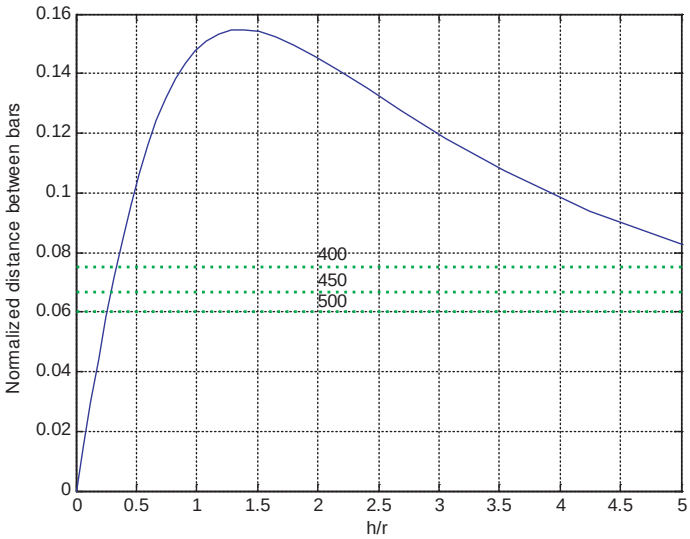

Figure 8. Clearance between bars. The horizontal lines indicate how the estimated required 30mm translates into normalized clearance for a given bar length.

Range of motion

Theoretically the structure can deform from a planar configuration with $h = 0$, to almost $h = b$. In reality, the components impose constraints on the practically possible range of motion. First, some assumptions need to be made about the components, before the analysis can be done. In our case the assumed value for the outer diameter of the bar with the springs, as well as the diameter of the flange, was set at 30mm.

spring elongation Due to the use of the pulley, for an untensioned spring, the elongation equals half of the length of the corresponding wire. These values are plotted as a ratio of the bar length in Fig. 7. As can be seen, the maximum practical elongation would be roughly 47% of the bar length. Assuming that the maximum elongation corresponds to 150% of rest length (which, as a rule of thumb, is the maximum allowed elongation), then for an untensioned spring with touching coils the rest length would be 31%, and the required distance between the flanges on the bar would thus have to be 78% of the bar length. Additionally some room is needed for attachment of spring, pulley and wires, estimated at 10mm at either end. These values determine a lower bound for the distance between the flanges, to achieve the maximal working range. If a non-maximal working range is sufficient, the distance can be adjusted accordingly, and reduced even further by using pretensioned springs.

contact between bars When the springs are attached alongside the bar, the effective outer diameter increases, and the springs of different bars might contact each other during displacement. The minimal distance between the centre lines of the bars is plotted as a function of h/r in Fig. 8. The horizontal lines in that figure indicate when the springs would collide for a given bar length, and thus show the restriction on the working range.

contact between wires and flange A more limiting factor is when the wires come in contact with the flanges; for a low h/r with the horizontal wires, and for a high h/r with the vertical wires. The flanges cannot be moved away from the endpoint indefinitely, as that would conflict with the required distance between the flanges to allow for the spring elongation. The angles between wires and bar can be calculated as a function of h/r, but more interesting is to show how far the flanges should be removed from the endpoint to just avoid contact. By then plotting the available distance from the endpoint of the bar for a given bar length, the available range of motion is found. See Fig. 9.

Using Fig. 9 the estimated working range for the final structure, with a bar length of 450mm, was found to be $h/r = [0.5 \ldots 4.5]$. Using Fig. 4 this corresponds to a height range of $[113 \ldots 415]$mm, and radius range of $[92 \ldots 225]$mm. This was deemed more than sufficient to demonstrate the properties of this type of structure. A remark is in order about the accuracy of the estimated working range. The calculations done on the working range assume the structure to be purely pin-jointed with zero-width bars and wires. In practice the wires do not exit the bar at the centre line, but at the bar radius. This reduces the accuracy of especially Fig. 9. Nevertheless, the above calculations provide a good indication.

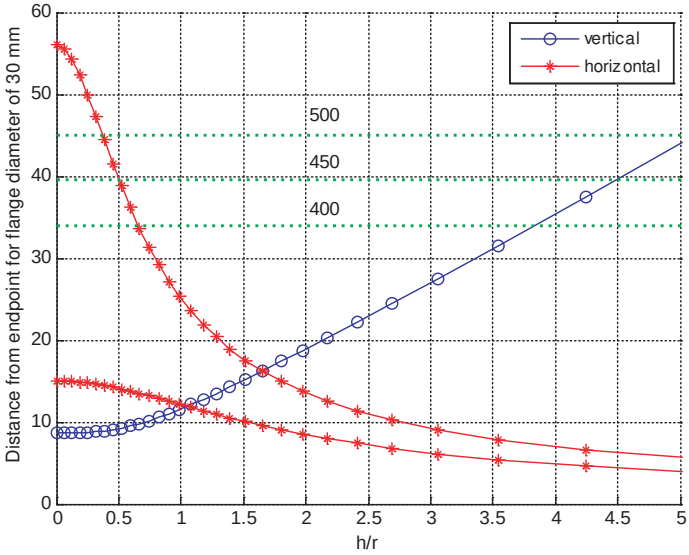

Figure 9. Distance from endpoint of the bar to flange, which just avoids contact between wire and flange, for a given flange diameter. The horizontal lines indicate the available length from the endpoint for various bar lengths (11% -10mm). The intersection of the horizontal line with the curves provides the working range.

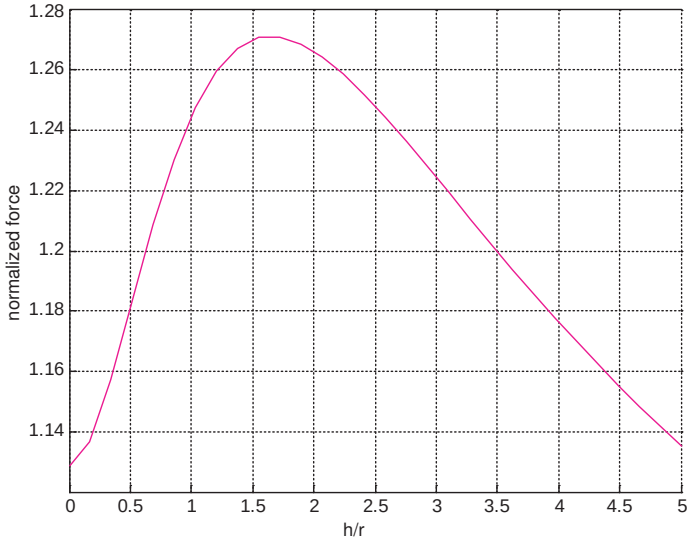

Figure 10. Normalized axial force, due to the elongation of the springs. When multiplied with the bar length and the horizontal spring stiffness, the total axial force is found.

As shown above, the main limitation on the working range is posed by the contact between flange and wires. This can be improved by moving the flanges away from the endpoint by choosing springs that can reach higher levels of elongation, and by reducing the diameter of the flanges by choosing smaller springs. This illustrates there is some leeway for optimization in future designs.

Miscellaneous

As mentioned earlier, theoretically the tension coefficient, and thus length, of the bar remains constant throughout displacement. This is true if zero-free-length springs are used which are attached from endpoint to endpoint of the bars. In the current setup, however, all springs exert axial forces on the bar, and the axial force is not constant throughout displacement. The maximum axial force exerted by the combined elongations of the springs can be calculated (see Fig. 10) and was checked with the buckling load of the bar.

Throughout the displacement, the angles the wires make with respect to each other change. As a result, the ideal attachment position of the springs along the circumference of the bar changes (see Fig. 11). The angles between the various wires are plotted in Fig. 12. A reference position was chosen which more or less gave an average angle between the extremes of the working range. Note that the changing angles mean that the bars rotate slightly around their axis during displacement.

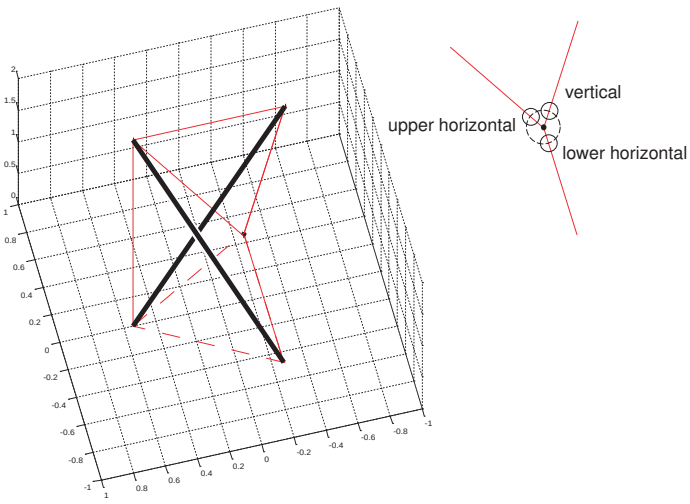

Figure 11. Angles between the various springs attached alongside the bar. Using Fig. 12 the angles between upper/vertical, vertical/lower, and upper/lower were respectively chosen as 90°, 125° and 145°.

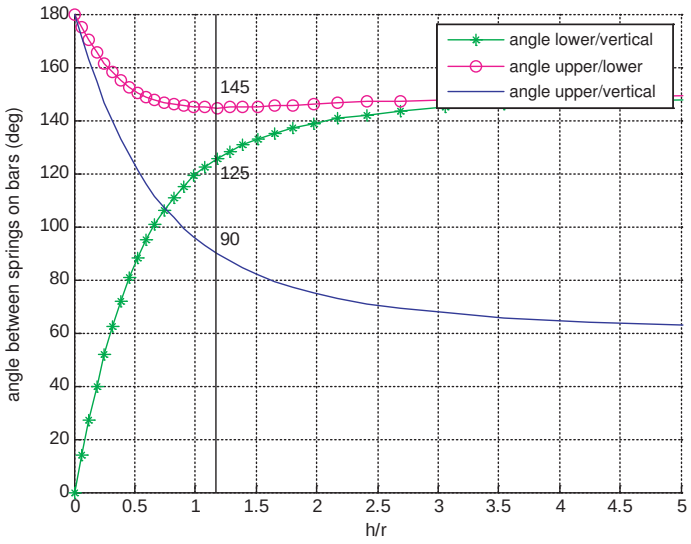

Figure 12. Angles between the wires corresponding to the springs attached alongside the bars. The vertical line indicates the chosen reference position.

As the structure is only in equilibrium when all springs are attached in the correct manner, the bars need to be firmly fixed during assembly. An important part of assembly is also to make sure that each spring is properly configured to emulate a zero-free-length spring. The assembly process will become more troublesome when the structures become more complex.

FINAL STRUCTURE

The final structure, shown in Fig. 13, can be deformed into a continuous range of positions whilst remaining in equilibrium. This includes non-symmetric configurations, due to the additional two zero-stiffness modes. The structure was not taken to the extremes of its working range, as for large extensions of the springs the wires would often slip out of the pulleys; this can be avoided by a more robust pulley design.

There is a substantial amount of friction in the system. The upside of the friction is that the structure does not collapse under its own weight, and that substantially less fine tuning was needed to assemble the structure. The downside is that the friction needs to be overcome when deforming, so although the structure has zero stiffness, it *does* require external work to deform. Another consequence of the friction is that the structure can be deformed into positions which should otherwise provide some stiffness. In that respect it does not faithfully demonstrate the properties of this type of mechanism.

CONCLUSIONS

We have designed and constructed a statically balanced tensegrity mechanism based on a classic tensegrity structure. It can be deformed into a wide range of positions, while remaining in equilibrium.

The distinguishing feature of this class of mechanisms is that, as a tensegrity, every member is stressed, and it is also the main source of difficulty when designing and constructing these systems. Tensegrity literature provides a lot of techniques for finding an initial equilibrium configuration (i.e. form finding) and the tools of structural engineering can be used to show if a tensegrity structure constructed with zero-free-length springs will indeed have zero stiffness, and is thus a mechanism. The next step in the process is to analyse the mechanism properties of the structure such as the range of motion. For this, the currently used method is to derive the analytical equilibrium equations, and investigate the structure by that means. This approach is somewhat limited as it only allows the analysis of fairly simple structures, and only part of the total behaviour: e.g. for the mechanism described in this paper only the symmetric deformation was analysed. The internal forces also require attention during assembly of the mechanism, as it will only be balanced when all springs are tensioned and until then it needs to be firmly fixed.

The design of the springs is key in these mechanisms. If the springs can achieve larger elongations, the working range can be increased. Appropriate (and accurately manufactured) spring stiffness ratios are also needed, and these are not always available in standard spring catalogues. When the friction is sufficiently reduced, the accuracy of the zero rest length of the springs becomes increasingly important and would require a lot of fine tuning. It is currently unclear how it would best be done, to determine which springs to adjust, and by how much.

Interesting unanswered (theoretical) questions, include that of the number of DOF of statically balanced tensegrity mechanisms. As the structures would be structurally stiff when constructed with conventional elements, any degrees of freedom are introduced by the zero-free-length springs (or equivalents), and are not covered by any definition of DOF known to the authors. Actuation of these mechanisms has also not been considered yet. To excite the entire system, multiple actuators are probably needed. It is also difficult to determine which of the zero-stiffness modes is actuated. Therefore it would be interesting to construct a rotationally symmetric model with 5 (or more) bars, as by [8] that would have only one zero-stiffness mode, and could possibly be actuated with only one actuator.

A lot of work is left to be done in this field, but the design of the prototype has already revealed interesting aspects of statically balanced tensegrity mechanisms.

REFERENCES

[1] Herder, J. L., 2001. “Energy-free systems. Theory, conception and design of statically balanced spring mechanisms”. PhD thesis, Delft University of Technology.

[2] French, M. J., and Widden, M. B., 2000. “The spring-and-

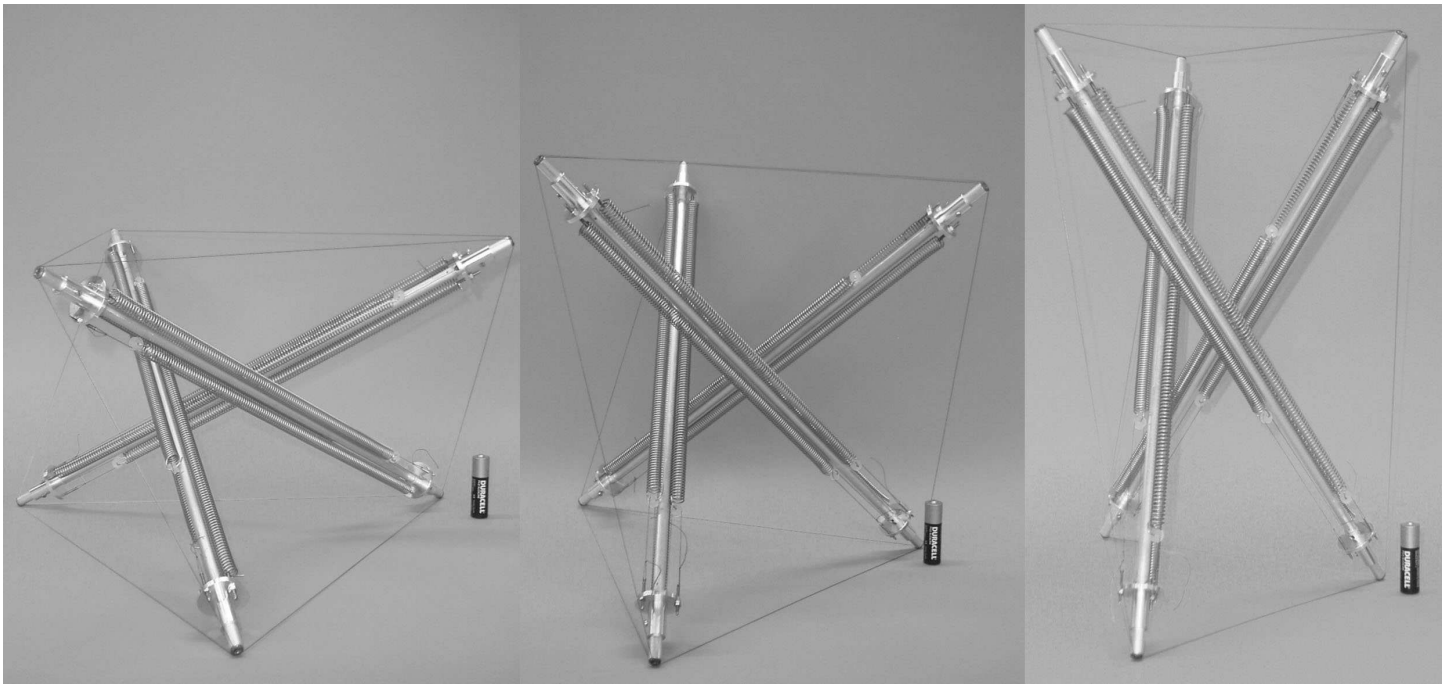

Figure 13. Illustration of the range of motion of the structure. Note that these positions do not represent the extremes of the working range, or the only possible deformation mode; further and other (asymmetric) deformation is still possible.

lever balancing mechanism, George Carwardine and the Anglepoise lamp". *Proceedings of the Institution of Mechanical Engineers part C – Journal of Mechanical Engineering Science*, **214**(3), pp. 501–508.

[3] Motro, R., 1992. "Tensegrity systems: The state of the art". *International Journal of Space Structures*, **7**(2), pp. 75–83.

[4] Buckminster Fuller, R., 1962. Tensile-integrity structures. US Patent Number 3,063,521, Nov. 13.

[5] Snelson, K. D., 1965. Continuous tension, discontinuous compression structures. US Patent Number 3,169,611, Feb. 16.

[6] Calladine, C. R., 1978. "Buckminster Fuller's 'tensegrity' structures and Clerk Maxwell's rules for the construction of stiff frames". *International Journal of Solids and Structures*, **14**, pp. 161–172.

[7] Pellegrino, S., and Calladine, C. R., 1986. "Matrix analysis of statically and kinematically indeterminate frameworks". *International Journal of Solids and Structures*, **22**(4), pp. 409–428.

[8] Schenk, M., Guest, S. D., and Herder, J. L., 2006. Zero Stiffness Tensegrity Structures. To be submitted to the International Journal of Solids and Structures.

[9] Connelly, R., and Terrell, M., 1995. "Globally rigid symmetric tensegrities". *Structural Topology*, **21**, pp. 59–77.

[10] Tibert, A. G., and Pellegrino, S., 2003. "Review of form-finding methods for tensegrity structures". *International Journal of Space Structures*, **18**(4), pp. 209–223.

[11] Murakami, H., 2001. "Static and dynamic analyses of tensegrity structures. Part II. Quasi-static analysis". *International Journal of Solids and Structures*, **38**, pp. 3615–3629.

[12] Masic, M., Skelton, R. E., and Gill, P. E., 2005. "Algebraic tensegrity form-finding". *International Journal of Solids and Structures*, **42**(16–17), pp. 4833–4858.

[13] Guest, S. D., 2006. "The stiffness of prestressed frameworks: A unifying approach". *International Journal of Solids and Structures*, **43**(3–4), pp. 842–854.

[14] Kangwai, R. D., and Guest, S. D., 1999. "Detection of finite mechanisms in symmetric structures". *International Journal of Solids and Structures*, **36**(36), pp. 5507–5527.

Appendix A: Analytical Equilibrium Conditions

Finding the initial equilibrium configurations for tensegrity structures, is referred to as form finding [10]. Rotationally symmetric, or prismic, tensegrities have been the object of study in the past and analytical equilibrium solutions exist [9, 11]. There are two general approaches to deriving the equilibrium conditions: statically and kinematically. The former works from nodal equilibria, the latter from the premise that in tensegrity structures the bar lengths reach a maximum and cable lengths a minimum. Here the static method is used.

Equilibrium configuration

The generic rotationally symmetric structure under consideration is depicted in Fig. 14. It consists of n bars, connecting the vertices of two regular n-polygons on two parallel planes, twisted over an angle α with respect to each other. The structure has height h, top radius r_h and bottom radius r_0. With these values all aspects of the structure can be calculated.

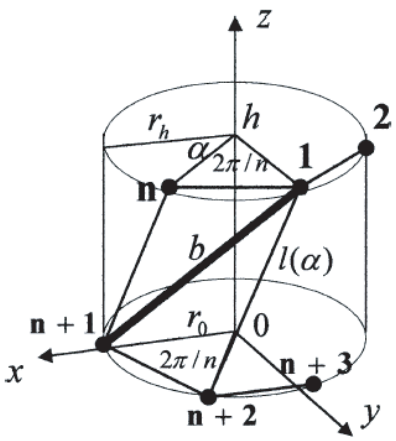

Figure 14. Rotationally symmetric tensegrity structure with n bars, height h, radii r_0 and r_h, and twist angle α. Figure copied from [11].

Element lengths. For the calculation of the element lengths, the cosine rule was used extensively:

$$c^2 = d^2 + e^2 - 2de\cos(\gamma). \tag{A.1}$$

With Eqn. A.1 the bar length b is then written as

$$b^2 = h^2 + r_0^2 + r_h^2 - 2r_0 r_h \cos(\frac{2\pi}{n} + \alpha), \tag{A.2}$$

the vertical cable length l as

$$l^2 = h^2 + r_0^2 + r_h^2 - 2r_0 r_h \cos(\alpha), \tag{A.3}$$

but the horizontal cable lengths l_0 and l_h are easier written as (with either r_0 or r_h):

$$l_0 = 2r_0 \sin(\frac{\pi}{n}). \tag{A.4}$$

Twist angle. In order to find the twist angle, we consider the nodal equilibrium at node $n+1$ in Fig. 14, with tension t_b in the bar, tension t_v in the vertical cable and t_0, t_h the tension in the bottom and top horizontal cables respectively.

First we consider equilibrium in the z-direction, which merely involves the vertical cable and bar:

$$\frac{t_b}{b}h + \frac{t_v}{l}h = 0 \tag{A.5}$$

which yields that

$$t_v = -\frac{t_b}{b}l. \tag{A.6}$$

Next the equilibrium in the y-direction is derived. Due to symmetry considerations on the horizontal cables, the contributions of the bar and vertical cable should cancel each other out. This analysis yields:

$$\sin(\alpha) r_h \frac{t_v}{l} + \sin(\frac{2\pi}{n} + \alpha) r_h \frac{t_b}{b} = 0 \tag{A.7}$$

which with Eqn. A.6 becomes

$$r_h \frac{t_b}{b}(\sin(\frac{2\pi}{n} + \alpha) - \sin\alpha) = 0. \tag{A.8}$$

For this to hold for any α we obtain

$$\sin(\frac{2\pi}{n} + \alpha) = \sin\alpha = \sin(\pi - \alpha) \tag{A.9}$$

and find that

$$\begin{aligned} \frac{2\pi}{n} + \alpha &= \pi - \alpha \\ 2\alpha &= \pi - \frac{2\pi}{n} \\ \alpha &= \frac{\pi}{2} - \frac{\pi}{n}. \end{aligned} \tag{A.10}$$

Note that the twist angle α only depends on n and is independent of the radius and height, and holds as long the structure is rotationally symmetric with two parallel n-polygons.

Equilibrium tensions

With the equilibrium twist angle now known, we wish to find the corresponding internal tensions. It was already shown in Eqn. A.6 that

$$t_v = -\frac{t_b}{b} l.$$

To calculate the tensions in the horizontal cables, the force equilibrium in x-direction at node $n+1$ is considered. The contributions of the vertical cable and bar to that equilibrium, $f_{x,vert}$, can be written as:

$$(r_0 - \cos\alpha r_h)\frac{t_v}{l} + \left(r_0 - \cos(\frac{2\pi}{n}+\alpha)r_h\right)\frac{t_b}{b} = f_{x,vert} \quad \text{(A.11)}$$

which, when using Eqn. A.6 becomes:

$$\left(\cos\alpha - \cos(\frac{2\pi}{n}+\alpha)\right) r_h \frac{t_b}{b} = f_{x,vert}. \quad \text{(A.12)}$$

With $\alpha = \frac{\pi}{2} - \frac{\pi}{n}$ we can write

$$\left(\cos(\frac{\pi}{2} - \frac{\pi}{n}) - \cos(\frac{\pi}{n} + \frac{\pi}{2})\right) r_h \frac{t_b}{b} = f_{x,vert} \quad \text{(A.13)}$$

and using the following goniometric relationships (with arbitrary β and γ)

$$\cos(\gamma+\beta) = \cos\gamma\cos\beta - \sin\gamma\sin\beta$$
$$\cos(\gamma-\beta) = \cos\gamma\cos\beta + \sin\gamma\sin\beta$$

we find

$$\left(\sin(\frac{\pi}{n}) + \sin(\frac{\pi}{n})\right) r_h \frac{t_b}{b} = f_{x,vert}$$
$$f_{x,vert} = 2\sin(\frac{\pi}{n}) r_h \frac{t_b}{b}. \quad \text{(A.14)}$$

Next, the effect of the tensions in the horizontal cables in the x-direction can be written as:

$$2\left(r_0 - \cos(\frac{2\pi}{n}) r_0\right)\frac{t_0}{l_0} = f_{x,horz}$$
$$f_{x,horz} = 2\left(1 - \cos(\frac{2\pi}{n})\right)\frac{r_0 t_0}{l_0}. \quad \text{(A.15)}$$

Now the two contributions are summed, and the solution to $f_{x,vert} + f_{x,horz} = 0$ yields:

$$\begin{aligned}
2\left(1-\cos(\tfrac{2\pi}{n})\right)\frac{r_0 t_0}{l_0} &= -2\sin(\tfrac{\pi}{n}) r_h \frac{t_b}{b} \\
\left(1-\cos(\tfrac{2\pi}{n})\right)\frac{r_0 t_0}{2r_0\sin(\frac{\pi}{n})} &= -\sin(\tfrac{\pi}{n}) r_h \frac{t_b}{b} \\
\left(1-\cos(\tfrac{2\pi}{n})\right) t_0 &= -2\sin^2(\tfrac{\pi}{n}) r_h \frac{t_b}{b} \\
\left(1-1+2\sin^2(\tfrac{\pi}{n})\right) t_0 &= -2\sin^2(\tfrac{\pi}{n}) r_h \frac{t_b}{b} \\
t_0 &= -r_h \frac{t_b}{b} \quad \text{(A.16)}
\end{aligned}$$

where use is made of

$$\cos(2\gamma) = 1 - 2\sin^2(\gamma). \quad \text{(A.17)}$$

Reasoning that in Eqn. A.16 the r_h has to be replaced by r_0 to obtain the tension t_h, all the tensions in the system can be written as follows:

$$[t_v \quad t_h \quad t_0] = -\frac{t_b}{b}[l \quad r_0 \quad r_h] \quad \text{(A.18)}$$

which corresponds to the results found by [11]. With some rewriting, the equilibrium equations can be written in terms of the tension coefficients:

$$\hat{t}_v = -\hat{t}_b \quad \text{(A.19)}$$
$$\hat{t}_b = -2\frac{r_h}{r_0}\sin\left(\frac{\pi}{n}\right)\hat{t}_h \quad \text{(A.20)}$$
$$\frac{\hat{t}_h}{\hat{t}_0} = \left(\frac{r_0}{r_h}\right)^2 \quad \text{(A.21)}$$

Spring stiffness ratio

In the analysis of statically balanced tensegrity mechanisms, the cables are replaced by zero-free-length springs. This leads to the question what the stiffness (ratios) of those springs must be in order to preserve equilibrium. With the spring stiffness of a zero-free-length spring equal to its tension coefficient, and with $r_0 = r_h = r$ and $\hat{t}_0 = \hat{t}_h = \hat{t}_{hor}$ we find that

$$\frac{K_{ver}}{K_{hor}} = \frac{\hat{t}_{ver}}{\hat{t}_{hor}} = \frac{2\sin\left(\frac{\pi}{n}\right)\hat{t}_{hor}}{\hat{t}_{hor}} = 2\sin\left(\frac{\pi}{n}\right) \quad \text{(A.22)}$$

and for our tensegrity prism with $n = 3$ we obtain:

$$\frac{K_{ver}}{K_{hor}} = 2\sin\left(\frac{\pi}{3}\right) = \sqrt{3}. \quad \text{(A.23)}$$